

# Observation of the lowest triplet transitions ${}^3\Sigma_g^+ - {}^3\Sigma_u^+$ in $\text{Na}_2$ and $\text{K}_2$

J. Huennekens, S. Schaefer, M. Ligare,<sup>a)</sup> and W. Happer

Department of Physics, Princeton University, Princeton, New Jersey 08544

(Received 5 December 1983; accepted 17 February 1984)

We report here the observation and definite identification of the lowest triplet transition  ${}^3\Sigma_g^+ - {}^3\Sigma_u^+$  in  $\text{Na}_2$  and  $\text{K}_2$ . The identification of these bands is based upon direct comparison of  $\text{K}_2$  absorption, thermal emission, and laser-induced fluorescence, and  $\text{Na}_2$  laser-induced fluorescence, with spectra calculated from recent, accurate, *ab initio* potential curves. These data also serve as a sensitive check on the accuracy of these potentials.

## I. INTRODUCTION

It is well known that diatomic alkali molecules possess two electronic states which separate at large  $R$  into two ground state atoms. The lower of these molecular states is the  ${}^1\Sigma_g^+$ , in which the spins of the two outermost electrons point in opposite directions. This state is bound by typically  $5000\text{ cm}^{-1}$  and is the lower electronic state in most of the well studied absorption spectra of these molecules. The other state  ${}^3\Sigma_u^+$ , in which the electron spins are aligned, is for the most part repulsive, although it has a very shallow van der Waals minimum. Comparatively little is known about this and higher triplet states since absorption out of the  ${}^3\Sigma_u^+$  state is weak due to the repulsive nature of the potential curve. Triplet bands are also difficult to study in laser-induced fluorescence since laser pumping mostly excites molecules in singlet states and the dipole selection rule  $\Delta S = 0$  precludes fluorescence to triplet levels. In the heavier alkalis, the  $\Delta S = 0$  selection rule breaks down, but the spectroscopy is more complicated due to the higher density of emission lines.

Since the  ${}^3\Sigma_u^+$  state is for the most part unbound, emission to this state should be a true continuum. Unstructured bands have in fact been discovered in the spectra of all the alkalis; the most widely studied being the sodium violet band<sup>1-7</sup> ( $\lambda = 416\text{--}457\text{ nm}$ ) and the potassium yellow band<sup>6-11</sup> ( $\lambda = 560\text{--}580\text{ nm}$ ). It is widely believed that these bands do constitute emission to the  ${}^3\Sigma_u^+$  states although conclusive evidence for this identification does not yet exist.

Interest in these triplet transitions is heightened by their "excimer" like nature, which Konowalow and Julienne<sup>12</sup> suggested may be used as a source of tunable, high-power lasers. In this regard, the lowest allowed triplet transitions, those from the  ${}^3\Sigma_g^+$  state of the first excited manifold (see Fig. 1) to the  ${}^3\Sigma_u^+$  state, are of particular interest because they are expected to occur in the near infrared where tunable lasers are scarce and somewhat troublesome to operate.

We report here new observations of the lowest  ${}^3\Sigma_g^+ - {}^3\Sigma_u^+$  bands of  $\text{Na}_2$  and  $\text{K}_2$  using the high-density alkali jet apparatus developed by Ligare *et al.*<sup>13,14</sup> In the case of sodium, this band was observed in laser-induced fluorescence, while for potassium we were able to observe this triplet band in absorption, thermal emission, and laser-induced fluorescence. The definite identification of these observed

bands as the  ${}^3\Sigma_g^+ - {}^3\Sigma_u^+$  bands is made by comparison of the observed spectra with spectra calculated using the *ab initio* potential curves recently obtained by Konowalow and co-workers.<sup>15-18</sup>

## II. THE EXPERIMENT

Figure 2 is a block diagram of the experimental apparatus. The alkali jet apparatus has been described in detail previously,<sup>13-14</sup> however, we include here a brief summary. Alkali metal boils in a stainless-steel boiler, and the vapor travels up a superheated chimney. As the vapor emerges from the chimney into the observation zone, it continues to be confined by a flowing annular sheath of hot argon gas. The argon flow is matched to that of the alkali vapor so that laminar flow and well defined boundaries are maintained throughout the observation region (a few centimeters in length). Beyond this point, the laminar flow breaks down and the argon and alkali enter cooler regions where the alkali condenses and is returned to the boiler under the influence of gravity. The argon is filtered and passes back to a noncontaminating bellows pump from which it recirculates. Running

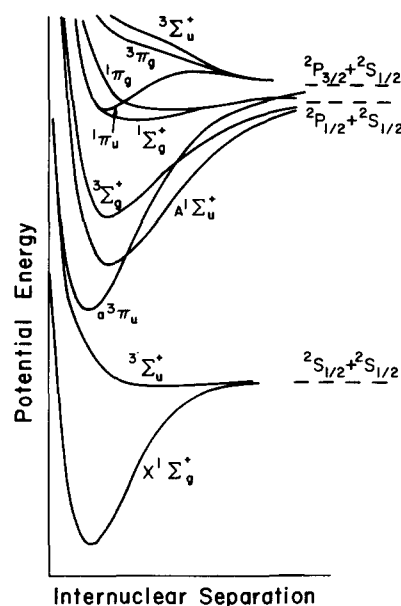


FIG. 1. Typical potential curves for homonuclear diatomic alkali molecules in the ground and first excited manifolds. These curves are only schematic and merely serve to indicate relative positions and qualitative shapes of the various potentials.

<sup>a)</sup>Current address: National Bureau of Standards, Building 221, Room A167, Washington, D.C. 20234.

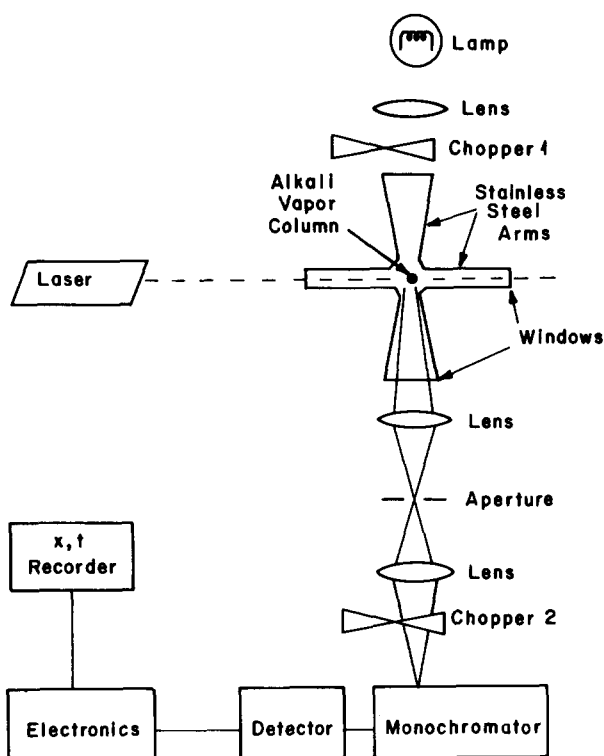


FIG. 2. Experimental setup.

time for this apparatus is presently limited to 5–10 h due to incomplete alkali condensation which causes a slow loss of metal to the argon filter. Planned modifications to the condensing section should increase running time significantly. The alkali column itself has been run at pressures up to 290 Torr and temperatures up to 750 °C for potassium, while for sodium we have worked at pressures up to 150 Torr and temperatures up to 850 °C. At these temperatures the dimer concentration is approximately 10% of the atom concentration.<sup>19</sup> The sharpness of the column boundaries is clearly visible to the naked eye if the vapor is illuminated from behind. The alkali vapor is deeply colored due to strong molecular absorption bands in the visible. The alkali column therefore stands out clearly against the surrounding transparent argon. The stability of the alkali column is demonstrated by the reproducibility and detail of the data (see Figs. 3–6 and Ref. 13).

Light emerging from the column is focused on an aperture (which limits the field of view to eliminate unwanted thermal radiation emitted by the hot stainless-steel surfaces) and then onto the slits of a 0.3 m monochromator. As detectors we have used photomultipliers with S-20 and S-1 cathode responses (EMI 9558 and RCA 7102), an intrinsic germanium near IR detector (North Coast E0-917L) and a PbS detector used in the photoconductive mode (Infrared Industries model 2767). For thermal spectra taken in the near IR using the S-1 photomultiplier, the current could be measured directly with a Keithley electrometer and then displayed on a chart recorder. Alternatively, or when using either the Ge or PbS detector, chopper 2 in Fig. 2 was used and lock-in detection employed. For absorption scans with any detector, chopper 1 was used and signals were detected

synchronously in order to discriminate against thermal radiation. For measurements of fluorescence induced by a cw laser (argon ion or oxazine dye pumped by a krypton ion laser), the laser was chopped and lock-in detection employed. Finally when either the 1.06 μm or frequency doubled 532 nm outputs of the pulsed Nd:YAG laser was used as the excitation source, we processed the laser-induced fluorescence signal with a gated box-car averager.

### III. RESULTS

Figure 3(a) shows the measured potassium absorption spectrum between  $\lambda = 0.8 \mu\text{m}$  and  $\lambda = 1.25 \mu\text{m}$ . For this scan, the potassium pressure was 290 Torr and the vapor temperature  $\sim 710 \text{ }^\circ\text{C}$ . As can be seen, almost complete absorption occurs for wavelengths less than  $\lambda \sim 1.06 \mu\text{m}$  which is the classical satellite of the  $A^1\Sigma_u^+ \leftarrow X^1\Sigma_g^+$  band. The absorption feature peaking at  $\lambda \sim 1.096 \mu\text{m}$  is the suspected  $^3\Sigma_g^+ \leftarrow ^3\Sigma_u^+$  satellite. The incomplete transmission beyond  $\lambda \sim 1.1 \mu\text{m}$  is believed to be simple scatter of incident light by small droplets in the jet. Figure 3(b) shows the absorption spectrum calculated from the recent *ab initio* K<sub>2</sub> potential curves of Konowalow and Fish.<sup>18</sup> Dipole moments were scaled asymptotically, to yield the experimental atomic dipole moment, from the Li<sub>2</sub> calculations of Ref. 17. Additionally the *R* scale for dipole moments was adjusted for the different ground state equilibrium separations in the two molecules. This scaling procedure is described in Ref. 16. The absorption spectrum was then calculated using the expression for the absorption coefficient

$$k_\nu(T) = \frac{4\pi^4\nu D^2 g^* n^2 [R(\nu)]^2}{|d\nu/dR|} e^{-\nu/kT}, \quad (1)$$

taken from quasistatic line broadening theory.<sup>20–22</sup> Here  $R(\nu)$  is the internuclear separation which yields the difference potential  $h\nu$ ,  $D$  is the transition dipole moment at the

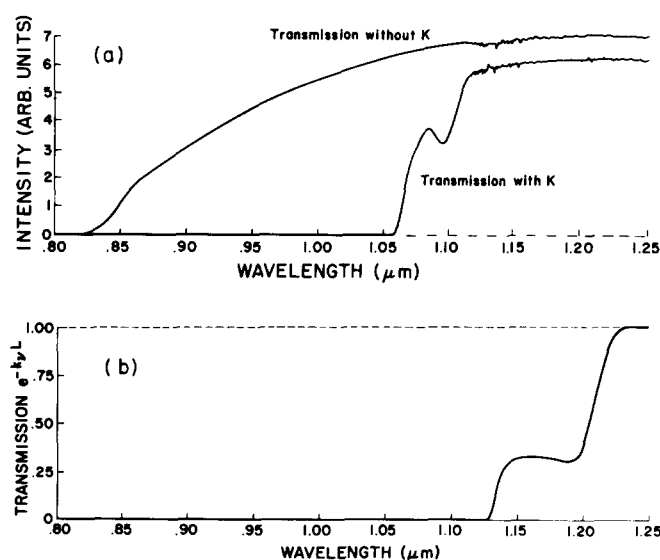


FIG. 3. (a) K<sub>2</sub> absorption spectrum between  $\lambda = 0.8$  and  $\lambda = 1.25 \mu\text{m}$  for potassium pressure of 290 Torr, vapor temperature of  $\sim 710 \text{ }^\circ\text{C}$ , and path length of 1 cm. The spectrum was obtained using the intrinsic Ge detector. (b) K<sub>2</sub> absorption spectrum ( $e^{-k_\nu L}$ ) in the same wavelength range, calculated from the potential curves of Ref. 18.

separation  $R$ ,  $V$  is the ground state potential at  $R$ ,  $g^*$  is the upper state statistical weight and  $n$  the atom density. Since Eq. (1) has a nonphysical singularity at the satellite where  $|dv/dR| \rightarrow 0$ , we have convoluted the absorption coefficient with a Gaussian of 20 nm full width at half-maximum. The statistical weights of the  $^3\Sigma_g^+$  and the  $^1\Sigma_u^+$  are 3 and 1, respectively. Equation (1) can be derived by realizing that

$$[D(R)]^2 (g^*/g) (8\pi^3 \nu / 3hc) \delta[\nu - \nu(R)] \\ = \frac{\pi e^2 f(R)}{mc} \delta[\nu - \nu(R)]$$

is the absorption cross section at  $R$  for each atom pair,  $n^2/2$  is the number of (identical) atom pairs,  $g/4$  is the probability that the atom pair is in the electronic ground state responsible for the absorption where  $g(^3\Sigma_u^+) = 3$ ,  $g(^1\Sigma_g^+) = 1$ , and  $4\pi R^2 dR e^{-V/kT}$  is the probability that the two atoms are separated by a distance  $R$  which yields absorption at frequency  $\nu$ . Multiplying the above terms together and integrating over values of  $\nu$  for each  $R$  then yields Eq. (1).

The calculated transmission spectrum shown in Fig. 3(b) is obtained from Eq. (1) as  $e^{-k_\nu L}$ , where  $L = 1$  cm is the path length through the vapor.

Figure 4(a) shows the K<sub>2</sub> near IR thermal emission spectrum at  $P = 290$  Torr and  $T = 710$  °C while Fig. 4(b) shows the thermal emission spectrum, calculated from the potential curves of Konowalow and Fish.<sup>18</sup> From Kirchhoff's law the thermal emission spectrum is related to the absorption spectrum by

$$I(\nu) = \epsilon_\nu I_{\text{BB}}(\nu), \quad (2)$$

where  $I_{\text{BB}}(\nu)$  is the emission spectrum of a perfect blackbody given by Planck's relation

$$I_{\text{BB}}(\nu) = \frac{8\pi h \nu^5}{c^4} [e^{h\nu/kT} - 1]^{-1} \quad (3)$$

and the emissivity  $\epsilon_\nu$  equals the absorptivity  $\alpha_\nu$  defined as

$$\epsilon_\nu = \alpha_\nu = 1 - e^{-k_\nu L}. \quad (4)$$

The thermal emission spectrum calculated from Eqs. (1)–(4), where  $k_\nu$  was again convoluted with a Gaussian of 20 nm width to smooth the satellites, is presented in Fig. 4(b). The

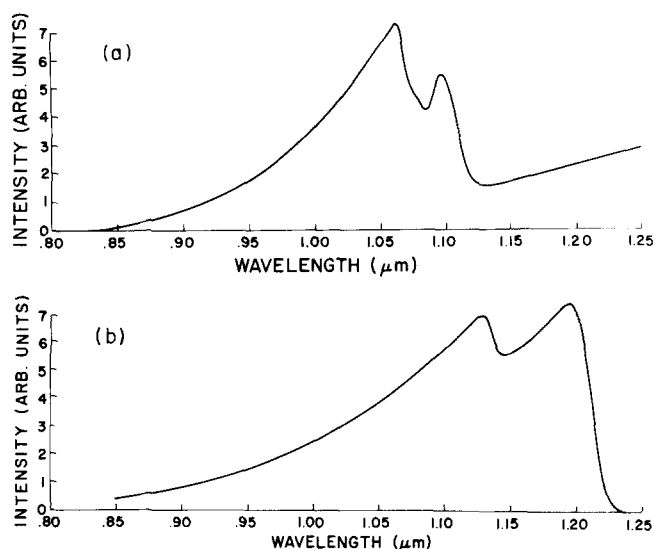


FIG. 4. (a) K<sub>2</sub> thermal spectrum between  $\lambda = 0.8$  and  $\lambda = 1.25$   $\mu\text{m}$  for potassium pressure of 290 Torr, vapor temperature of  $\sim 710$  °C, and column thickness of 1 cm. The spectrum was obtained using the intrinsic Ge detector. (b) K<sub>2</sub> thermal spectrum in the same wavelength range calculated from the potential curves of Ref. 18.

raw data in Figs. 3(a) and 4(a) were not corrected for relative detection system efficiency as a function of wavelength although this was only a 10%–20% effect (based on manufacturers specifications) over the range of interest (1.00–1.25  $\mu\text{m}$ ). Again the nonzero thermal emission at wavelengths longer than the triplet band satellite is thought to be scatter of blackbody emission from the walls by small droplets in the jet.

Figure 5 shows the near IR K<sub>2</sub> fluorescence spectrum excited by the Ar<sup>+</sup> laser line at 457.9 nm. This laser line excites the K<sub>2</sub> C ← X band. However, collisional mechanisms result in population of both the  $^3\Sigma_g^+$  and  $^1\Sigma_u^+$  states. Fluorescence from both of these states as well as from the B  $^1\Pi_u$  (0.65–0.76  $\mu\text{m}$ ) and several atomic lines is visible in the figure.

Figure 6(a) shows the near IR Na<sub>2</sub> fluorescence spectrum excited by the frequency doubled (532 nm) pulsed

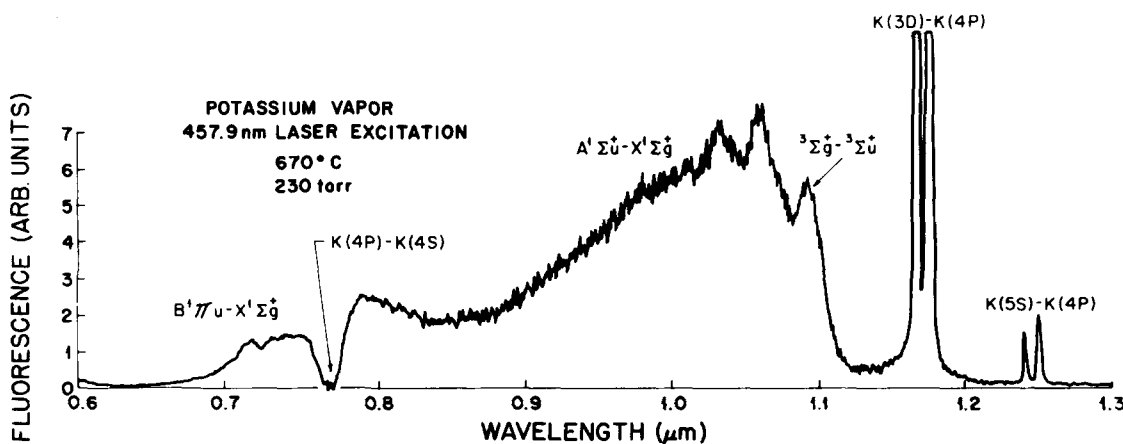


FIG. 5. K<sub>2</sub> fluorescence induced by 457.9 nm Ar<sup>+</sup> laser excitation for  $\lambda = 0.6$  to 1.3  $\mu\text{m}$ .  $P = 230$  Torr.  $T = 670$  °C. The spectrum was obtained using the photomultiplier with S-1 cathode response. The atomic lines to the red of the triplet satellite are due to ionization followed by recombination.

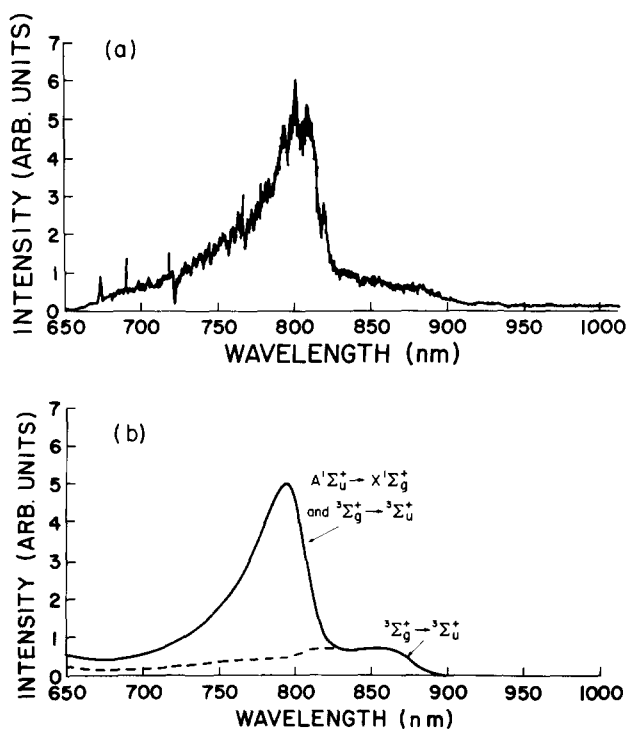


FIG. 6. (a) Na<sub>2</sub> fluorescence induced by the 532 nm frequency-doubled output of a Nd:YAG laser for  $\lambda = 0.65$  to  $1.00 \mu\text{m}$ .  $P = 96.5$  Torr.  $T = 769^\circ\text{C}$ . The spectrum was obtained using the photomultiplier with S-1 cathode response. (b) Na<sub>2</sub> "thermal" emission calculated from the potential curves of Refs. 15 and 17 for  $T_{\text{eff}} = 3700$  K.

Nd:YAG laser line (which excites the  $B^1\Pi_u \leftarrow X^1\Sigma_g^+$  Na<sub>2</sub> band). With the laser blocked, we found that the purely thermal contribution to this spectrum was less than 4% at all wavelengths. Figure 6(b) shows for comparison the spectrum calculated from the potential curves and transition moments of Konowalow, Rosenkrantz, and Olson<sup>15</sup> and Konowalow, Rosenkrantz, and Hochhauser.<sup>17</sup> In this case, we have not used expression (2) for the spectrum since the vapor column is not in thermal equilibrium. Instead we have used the expression

$$I(\nu) \propto g^* \left(\frac{\nu}{\nu_0}\right)^4 \frac{R^2(\nu)}{|d\nu/dR|} D^2 e^{-\nu^*/kT_{\text{eff}}} \quad (5)$$

for the emission, which is taken from the quasistatic line broadening theory.<sup>23</sup> We have again smoothed the classical satellites by convolution with a Gaussian of 20 nm width. We have also corrected this spectrum for self-absorption by multiplying  $I(\nu)$  by  $e^{-k\nu L/2}$ , obtained as in the K<sub>2</sub> case, which is the probability that photons emitted from the laser excited region will pass through the unexcited vapor in the detection direction without being absorbed. Additionally, since collisions are not frequent enough to completely thermalize the excited state populations, we have allowed the excitation temperature to be a free parameter in the calculations, which is varied to give a good match to the observed spectrum.

#### IV. DISCUSSION

Over the last few years, several diffuse bands have been observed in the spectra of diatomic alkali molecules includ-

ing the Na<sub>2</sub> violet band<sup>1-7</sup> (416–457 nm), the K<sub>2</sub> yellow band<sup>6-11</sup> (560–580 nm), and the three narrow peaks observed in the Cs<sub>2</sub> spectrum near 720 nm.<sup>24</sup> These bands are now all thought to be due to transitions to the repulsive  $^3\Sigma_u^+$  states from triplet levels lying above the first excited manifold. However, although this identification is reasonable and probably correct, very little hard evidence exists, either theoretical or experimental, in support of this conclusion. The best evidence to date for identifying any of these bands as a triplet, is the temperature dependence of the Cs<sub>2</sub> 720 nm band absorption which suggests a repulsive lower state.<sup>24</sup> (We have also studied the temperature dependences of the K<sub>2</sub> 570 nm and 1.1  $\mu\text{m}$  absorption bands in the high-density alkali jet apparatus, and found the results to be inconclusive. A detailed study of these effects will be possible with a planned second model of the alkali jet apparatus which will allow more effective decoupling of the boiler and chimney temperatures permitting independent control of the temperature and pressure of the vapor.)

In the case of the lowest triplet bands  $^3\Sigma_g^+ \rightarrow ^3\Sigma_u^+$ , which we report here, their identification rests on direct comparison to spectra calculated from accurate *ab initio* potential curves. Here the most sensitive comparison is probably that of the K<sub>2</sub> thermal emission spectrum for which an accurate calculation of the absorption coefficient is made, and the thermal emission obtained from Kirchoff's law. (The ability to obtain high temperature thermal emission spectra is a major advantage of the alkali vapor jet apparatus used here.) We find that the predicted band positions and satellite wavelengths, band shapes, and relative intensities of the  $A^1\Sigma_u^+ \rightarrow X^1\Sigma_g^+$  and  $^3\Sigma_g^+ \rightarrow ^3\Sigma_u^+$  bands agree fairly well with observations (see Fig. 4). The absorption spectrum (Fig. 3) also shows good agreement between the calculation and experiment especially considering there are no adjustable parameters in the calculated spectrum.

In the case of sodium, the triplet band is not observed either in absorption or thermal emission. This too agrees with the calculations which indicate that in thermal emission the triplet satellite intensity should only be  $\sim 1\%$  of the  $A$  band satellite intensity, and that in absorption the triplet satellite occurs at an internuclear separation  $R$  where the lower state potential curve is  $\sim 3$  kT repulsive (in K<sub>2</sub> the equivalent satellite position occurs where the lower state is only  $\sim 0.3$  kT repulsive). We can, however, still compare the Na<sub>2</sub> laser induced fluorescence to a calculated emission spectrum. In this case, since the laser pumps the  $B^1\Pi_u$  state, both the  $A^1\Sigma_u^+$  and the  $^3\Sigma_g^+$  states are populated collisionally. We therefore expect energy to be distributed in the  $A$  and triplet states in a quasithermal equilibrium. We expect, however, that because the  $B$  state lies above the  $A$  and triplet states, the effective excitation temperature will be significantly above the vapor temperature. In this regard, we can only say that the effective excitation temperature of 3700 K, which gives the best fit to the data (see Fig. 6), does not appear unreasonable. Again the band positions, satellite wavelengths, and band shapes are strong verification of this identification of the triplet band.

The present observations must rule out the tentative identification by Bhaskar *et al.*<sup>25</sup> of the weak absorption

bands observed in all the alkalis beyond  $1\ \mu\text{m}$ <sup>25-29</sup> as the lowest triplet transitions. (In the present experiment, we do not see these weak absorption bands because the scattering by small droplets is much more intense. That the long wavelength scatter we see can be attributed to droplets is supported by its wavelength independence and its absence in the Bhasker experiment.) In K<sub>2</sub> the weak absorption observed by Bhaskar *et al.* extends out to almost  $1.6\ \mu\text{m}$  and does not seem to be due to small droplets or fog, etc. With the present identification of the triplet bands, these weak absorption bands must be most likely attributed to trimers or higher polymers. Further work on these IR absorption bands is planned in this laboratory.

Once we have established the identification of these triplet bands, we can use these observations as a fairly sensitive test of the *ab initio* potential curves of Konowalow and co-workers. For example, calculated Na<sub>2</sub> *A-X* and triplet band satellite wavelengths are found to agree with the present observations to within 1% and 2%, respectively. (The recent Na<sub>2</sub> potential curves of Jeung,<sup>30</sup> which appeared as this paper was submitted, yield *A-X* and triplet band satellite wavelengths which agree even more closely, i.e., well within 1%, with our data.) Similarly in K<sub>2</sub>, the calculated *A-X* and triplet satellite positions based on the Konowalow potentials, differ from experiment by  $\sim 7\%$  and  $9\%$ , respectively. The larger discrepancies in the K<sub>2</sub> case reflect the increased difficulty of the calculations for heavier molecules. Additionally the calculated absolute magnitude of the K<sub>2</sub> triplet band satellite absorption coefficient agrees with our measurements to within 50%. This agreement is remarkable considering the calculation of the absorption coefficient contains no adjustable parameters.  $k_\nu$  depends on the square of the scaled dipole transition moments  $D$  and on the square of the potassium density  $n$ . In fact a lowering of the product  $Dn$  by only 27% in the calculation would bring the experiment and calculation into almost complete agreement. This is just outside experimental uncertainties, the most significant of which is probably the vapor temperature in the observation zone which is taken from readings of thermocouples attached to the outside of the stainless-steel chimney. In view of these experimental uncertainties, and the approximations involved in the calculation of the spectrum from the quasistatic theory and in the Gaussian convolution, we believe the overall agreement between experiment and calculation is quite good. The relative intensities of the calculated K<sub>2</sub> *A-X* and triplet band thermal emission also agrees with our data to within 35%. This discrepancy in relative intensity can be explained in part by the fact that the wavelength splitting between the two satellites is larger in the calculated spectrum than in the experimental spectrum. Convolution with the blackbody spectrum (3) thus enhances the triplet satellite relative to the singlet emission in the calculated spectrum by a factor of 1.14. Uncertainties in the experiment and calculation are more than sufficient to account for remaining discrepancies. Woerdman and de Groot<sup>21,22</sup> also found very good agreement between observed absorption spectra for the Na<sub>2</sub> bands  ${}^3\Pi_g \leftarrow {}^3\Sigma_u^+$ ,  ${}^1\Pi_u \leftarrow {}^1\Sigma_g^+$ , and  ${}^1\Sigma_u^+ \leftarrow {}^1\Sigma_g^+$  and those calculated from the Konowalow *et al.*<sup>15-17</sup> potential curves. Thus the accuracy of these potential

curves seems well established.

Prior to our initial report in Refs. 13 and 14 of the IR spectrum of dense potassium vapor, all previous observations in this spectral region were taken from electric discharges.<sup>31,32</sup> Although the  ${}^3\Sigma_g^+ \leftarrow {}^3\Sigma_u^+$  is probably contributing to these spectra, the stark broadened atomic 5F-3D transition at  $1.10\ \mu\text{m}$  complicates the identification. These atomic levels are not populated under the conditions in which our absorption and thermal emission spectra were taken. With the aid of the recent potential curves of Konowalow and co-workers, the Na<sub>2</sub>  ${}^3\Sigma_g^+ \leftarrow {}^3\Sigma_u^+$  band can be identified in Fig. 4 of Ref. 31 and Fig. 4 of Ref. 32. Shahdin *et al.*<sup>33</sup> also observed this Na<sub>2</sub> laser-induced fluorescence in a heat pipe oven and identified it as the  ${}^3\Sigma_g^+ \leftarrow {}^3\Sigma_u^+$  band based on a comparison of observed wavelengths with those predicted by Konowalow *et al.*<sup>15</sup> The present detailed comparison of emission intensity versus wavelength confirms this identification. Additionally, Sorokin and Lankard<sup>32</sup> took high resolution Na<sub>2</sub> data which indicates that the emission plateau between 800 and 900 nm, which we here definitely identify as the  ${}^3\Sigma_g^+ \rightarrow {}^3\Sigma_u^+$  emission, is a true continuum, consistent with this interpretation.

## V. CONCLUSIONS

We report here the observation of the lowest K<sub>2</sub> triplet band  ${}^3\Sigma_g^+ \leftarrow {}^3\Sigma_u^+$  in absorption, thermal emission, and laser-induced fluorescence, and also observation of the analogous Na<sub>2</sub> band in laser-induced fluorescence. The identification of the bands is made by detailed comparisons to spectra calculated from the *ab initio* potentials of Konowalow and co-workers.<sup>15-18</sup> The comparison also serves as sensitive test of these potential curves, and their consistency with the present observations is extremely satisfactory.

The identification of these excimer-like bands is the first step in producing tunable, near IR lasers based on these transitions. Work toward this end is currently underway in our laboratory. We are encouraged in this endeavor by the recent observations of enhanced fluorescence along the pump laser axis, by Wu *et al.*<sup>34</sup> and of gain by Bahns and Stwalley<sup>35</sup> in the Na<sub>2</sub> violet bands.

*Note added in proof:* Recent work by L. Li and R. W. Field [J. Phys. Chem. **87**, 3020 (1983)] has identified the upper state of the sodium violet band as  ${}^3\Pi_g$  using optical-optical double resonance fluorescence excitation spectroscopy. Additionally, G. Pichler, S. Milosevic, D. Veza, and R. Beuc [J. Phys. B **16**, 4619 (1983)] have demonstrated, through temperature dependent absorption studies, that the sodium violet and potassium yellow bands are in fact transitions involving the repulsive  ${}^3\Sigma_u^+$  state.

## ACKNOWLEDGMENTS

We would like to thank Dr. D. D. Konowalow for making the results of his calculations available to us prior to publication. We would also like to thank Dr. Robert Austin and Dr. Jane LeGrange for use of their Nd:YAG laser and for assistance in its operation. This work was supported under grants DAAG-29-81-K-0011 and DAAG-29-83-K-0072 from the U.S. Army Research Office.

- <sup>1</sup>M. Allegrini, G. Alzetta, A. Kopystynska, L. Moi, and G. Orriols, *Opt. Commun.* **22**, 329 (1977).
- <sup>2</sup>J. P. Woerdman, *Opt. Commun.* **26**, 216 (1978).
- <sup>3</sup>A. Kopystynska and P. Kowalczyk, *Opt. Commun.* **28**, 78 (1979).
- <sup>4</sup>M. Allegrini and L. Moi, *Opt. Commun.* **32**, 91 (1980).
- <sup>5</sup>C. Y. R. Wu and J. K. Chen, *Opt. Commun.* **44**, 100 (1982).
- <sup>6</sup>G. Pichler, S. Milosevic, D. Veza, and S. Bosanac, in *Spectral Line Shapes*, edited by K. Burnett (Walter de Gruyter, Berlin, 1983), Vol. 2, p. 613.
- <sup>7</sup>Cz. Radzewicz, P. Kowalczyk, and J. Krasinski *Opt. Commun.* **44**, 139 (1983).
- <sup>8</sup>J. M. Walter and S. Barratt, *Proc. R. Soc. London, Ser. A* **119**, 257 (1928).
- <sup>9</sup>M. M. Rebeck and J. M. Vaughan, *J. Phys. B* **4**, 258 (1971).
- <sup>10</sup>Yu. P. Korchevoi, V. I. Lukashenko, and S. N. Lukashenko, *Sov. Phys. JETP* **48**, 428 (1978).
- <sup>11</sup>Yu. P. Korchevoi, V. I. Lukashenko, and S. N. Lukashenko, *Phys. Scr.* **19**, 271 (1979).
- <sup>12</sup>D. D. Konowalow and P. S. Julienne, *J. Chem. Phys.* **72**, 5815 (1980).
- <sup>13</sup>M. Ligare, S. Schaefer, J. Huennekens, and W. Happer, *Opt. Commun.* **48**, 39 (1983).
- <sup>14</sup>M. Ligare, Ph.D. thesis, Columbia University, 1983 (unpublished).
- <sup>15</sup>D. D. Konowalow, M. E. Rosenkrantz, and M. L. Olson, *J. Chem. Phys.* **72**, 2612 (1980).
- <sup>16</sup>D. D. Konowalow and M. E. Rosenkrantz, in *Metal Bonding and Interactions in High Temperature Systems*, edited by J. L. Gole and W. C. Stwalley, ACS Symposium, Series 179 (American Chemical Society, Washington, D.C., 1982), p. 3.
- <sup>17</sup>D. D. Konowalow, M. E. Rosenkrantz, and D. S. Hochhauser, *J. Mol. Spectrosc.* **99**, 321 (1983).
- <sup>18</sup>D. D. Konowalow and J. L. Fish (to be published).
- <sup>19</sup>A. N. Nesmeyanov, *Vapor Pressure of the Elements* (Academic, New York, 1963).
- <sup>20</sup>L. K. Lam, A. Gallagher, and M. M. Hessel, *J. Chem. Phys.* **66**, 3550 (1977).
- <sup>21</sup>J. P. Woerdman and J. J. de Groot, *Chem. Phys. Lett.* **80**, 220 (1981).
- <sup>22</sup>J. P. Woerdman and J. J. de Groot, in *Metal Bonding and Interactions in High Temperature Systems*, edited by J. L. Gole and W. C. Stwalley, ACS Symposium, Series 179 (American Chemical Society, Washington, D.C., 1982), p. 33.
- <sup>23</sup>A. Gallagher, in *Atomic Physics 4*, edited by G. zu Putlitz, E. W. Weber, and A. Winnacker (Plenum, New York, 1975), p. 559.
- <sup>24</sup>R. Gupta, W. Happer, J. Wagner, and E. Wennmyr, *J. Chem. Phys.* **68**, 799 (1978).
- <sup>25</sup>N. D. Bhaskar, E. Zouboulis, T. McClelland, and W. Happer, *Phys. Rev. Lett.* **42**, 640 (1979).
- <sup>26</sup>V. E. Chertoprud, *Teplofiz. Vys. Temp.* **14**, 216 (1976) [*High Temp.* **14**, 195 (1976)].
- <sup>27</sup>E. Zouboulis, N. D. Bhaskar, A. Vasilakis, and W. Happer, *J. Chem. Phys.* **72**, 2356 (1980).
- <sup>28</sup>A. Vasilakis, N. D. Bhaskar, and W. Happer, *J. Chem. Phys.* **73**, 1490 (1980).
- <sup>29</sup>A. Vasilakis, Ph.D. thesis, Columbia University, 1981 (unpublished).
- <sup>30</sup>G. Jeung, *J. Phys. B* **16**, 4289 (1983).
- <sup>31</sup>K. Schmidt, in *Comptes Rendus de la VI<sup>e</sup> Conférence Internationale sur les Phénomènes d' Ionisation dans les Gaz, Vol. III*, edited by P. Hubert and E. Crémieu-Alcan (S.E.R.M.A., Paris, 1963), p. 323.
- <sup>32</sup>P. P. Sorokin and J. R. Lankard, *J. Chem. Phys.* **55**, 3810 (1971).
- <sup>33</sup>S. Shahdin, B. Wellegehausen, and Z. G. Ma, *Appl. Phys. B* **29**, 195 (1982).
- <sup>34</sup>C. Y. R. Wu, J. K. Chen, D. L. Judge, and C. C. Kim, *Opt. Commun.* **48**, 28 (1983).
- <sup>35</sup>J. T. Bahns and W. C. Stwalley *Appl. Phys. Lett.* (in press).